

A hierarchical Bayesian integrated model incorporated direct ageing,  
mark-recapture and length-frequency data for yellowfin (*Thunnus albacares*)  
and bigeye (*Thunnus obesus*) of the Indian Ocean

Dortel E.<sup>1</sup>, Sardenne F.<sup>2</sup>, Le Croizier G.<sup>2</sup>, Million J.<sup>3</sup>, Hallier J.P.<sup>1</sup>, Morize E.<sup>2</sup>  
Munaron J.M.<sup>2</sup>, Bousquet N.<sup>4</sup>, Chassot E.<sup>1</sup>

<sup>1</sup> *Institut de Recherche pour le Développement, UMR 212 EME, Avenue Jean Monnet, BP 171, 34 203 Sète cedex, FRANCE*

<sup>2</sup> *Institut de Recherche pour le Développement, UMR 6539 LEMAR, BP70, 29 280 Plouzané, FRANCE*

<sup>3</sup> *Indian Ocean Tuna Commission, PO Box 1011, Victoria, SEYCHELLES*

<sup>4</sup> *EDF Research and Development, Department of Industrial Risk Management, 6 quai Watier, 78 401 Chatou, FRANCE*

*Abstract.* Despite several studies conducted in the 3 oceans, the shape and parameterization of yellowfin and bigeye growth curves are still open to debate. In this study, we present an integrated growth model that combines mark-recapture and direct ageing data from saggital otoliths collected through the Indian Ocean Tuna Tagging Program (RTTP-IO) and the West Sumatra Tuna Tagging Project (WSTTP) as well as length-frequency data sampled from the European purse seine fishery over the last decade. Developed in a Bayesian framework, the model accounts for uncertainty in age estimates and includes ancillary information derived from expert judgment on otolith reading as well as from data on sex and observed maximum size of fish individuals. Our results confirm the existence of 2 stanzas for the growth of yellowfin and bigeye during exploitation phase.

*Key words:* Yellowfin; Bigeye; integrated growth model; Bayesian framework

# 1 Introduction

Fish growth is a key biological parameter in fisheries research. Determining mean population growth as well as variability among individuals are essential to understand the productivity of fish populations and their ability to resistance to environmental change and fishing pressure. Growth curves are used as input, directly or indirectly, into the stock assessment models to estimate the age composition of the commercial catches and supply the scientific advice on stock status.

Different sources of information for studying fish growth are available, (i) direct ageing of a fish of known size from periodic deposits in calcified and skeletal tissues, such as scales, vertebrae, otoliths, and spines, (ii) increase in fish length over the time at liberty from mark-recapture experiments, (iii) modal progressions in lengthfrequency distributions from commercial catches or scientific monitoring. These different data sources provide additional informations on different life cycle stages and therefore on growth phases and it may be difficult to obtain an overall growth pattern from a single data source. However, although many studies have been conducted on fish growth, however, only few studies have attempted to combine the different information sources in an integrated growth model (Eveson et al., 2004; ?).

Yellowfin tuna (*Thunnus albacares*) and bigeye tuna (*Thunnus obesus*) are epipelagic species widely distributed in the tropical and subtropical waters of the major oceans. In the Indian Ocean (IO), these tuna stocks are exploited by a large diversity of fishing fleets from industrial fleets dominated by longline and purse seine to artisanal fleets (Herrera and Pierre, 2010) and the induced effects are very important for the economic development of Indian coastal States. Therefore, it is necessary to conciliate a sustainable management of the stock with the economic constraints encountered by these countries.

The management anervation of Indian Ocean tunas are uner the jurisdiction of he Indian Ocean Tuna Commission (IOTC) and relies on the assessment of the stock status through age-structured population dynamics models (Langley et al., 2010). The age-structure in commercial fisheries catches is assess from the length-structure using an age-length key derived from growth parameters. Nevertheless, much uncertainty currently remains on the growth to be considered in yellowfin and bigeye stock assessments. Growth of the Indian Ocean yellowfin has been the focus of several studies based on modal progression analysis (Marsac and Lablache, 1985; Marsac, 1991; Lumineau, 2002; Viera, 2005) and direct ageing (Le Guen and Sakagawa, 1973; Romanov and Korotkova, 1988; Stéquer, 1995) leading to conflicting results due to differences in sampling, gear selectivity, and estimation methods historically raised issues about the shape of the growth curve and its parameterization. Historical studies on yellowfin growth relied on the classical Von Bertalanffy model (1938), assuming a constant growth rate over the full lifespan of the fish, while most recent studies support a two-stanza growth curve characterized by a significant change in growth rate between juveniles and adults (Gascuel et al., 1992; Lehodey and Leroy, 1999; Lumineau, 2002). In addition, modal progression and direct ageing data have specific features and biases, which makes difficult the comparison of growth curves obtained from a single data source. Growth bigeye has been little

study (Chantawong et al., 1999; Stéguert and Conand, 2004) and remain poorly known. Preliminary studies of data collected throughout the RTTP-IO, including otolith and tag-recapture, supported a two-stanza growth pattern both for yellowfin and for bigeye characterized by a slowdown during their juvenile phase (?).

Most stock assessments consider a mean growth pattern and static parameter estimates. The range of uncertainty as well as individual variability are ignored which result in substantial biases in estimates of stock productivity or stock resilience to fishing (Punt and Hilborn, 1997) and eventually modify the perception of stock status and associated management advice. The first source of variability in growth might arise from a sexual dimorphism. For Indian Ocean yellowfin, several authors showed that males become largely dominant above 145 cm  $F_L$  (Nootmorn et al., 2005; Zhu et al., 2008; Zudaire et al.). According to Wild (1986), in the eastern Pacific, the yellowfin females faster growth than the male until 94.9 cm  $F_L$  (at about 2 years) then the trend reverses. For Pacific Ocean bigeye, the ratio of males increases from 120 cm  $F_L$  and reached 75% over 170 cm (Kume and Joseph, 1966). Since the 1990s, Bayesian modelling approaches have gained growing interest in applied ecology and environmental sciences (Clark, 2005). The Bayesian framework offers the advantage of incorporating into the statistical data analysis some expert judgment and ancillary information in a rigorous and consistent manner (Gelman et al., 2004; Cressie et al., 2009). This is particularly suitable in fisheries science where data are almost always partially observed with measurement errors or uncertainties. Bayesian models have been used to make inferences about fish growth (Helser and Lai, 2004) so as to provide scientific advice for fisheries management (Punt and Hilborn, 1997; McAllister et al., 2001; Chen et al., 2003).

In this study, we present an integrated growth model that combine mark-recapture and otolith readings collected through the Indian Ocean Tuna Tagging Program (RTTP-IO), as well as otoliths collected during the West Sumatra Tuna Tagging Project (WSTTP), and length-frequency data sampled from the European purse seine fishery over the last decade. Developed in a hierarchical Bayesian framework, a flexible approach to exploit diverse sources of information that complement each, the model accounts for uncertainty in age estimates and length measurements and includes ancillary information derived from expert judgment on otolith reading. In a first part, the integrated model is used to provide robust estimates of growth of Indian Ocean yellowfin and bigeye tunas. Then, the model results are used to highlight a sexual dimorphism of growth from a sub-sample of data.

## 2 Materials and Methods

### 2.1 Data collection

#### 2.1.1 Mark-recapture data

Mark-recapture data were collected throughout the Regional Tuna Tagging Project (RTTP-IO). This tagging were carried out by IOTC during 2005-2007 on 3 pole-and-line vessels chartered to

operate in the Western Indian Ocean and off western Indonesia. In addition, from 2002 to 2009, the IOTC released 31,455 tunas during one-shot operations (Maldives, Laccadive, Andaman, Indonesia, Mayotte, Eastern Indian Ocean). Field operations consisted in catching tunas, tagging them on a vinyl-covered cradle, measuring their fork length (fish length from the front to the fork in the center of the tail;  $F_L$ ) through graduations directly printed on the cradle and releasing them at sea (Hallier, 2008). Date and geographic location were recorded for each tag event. A total of 64,323 yellowfin and 34,960 bigeye were tagged with Hallprint<sup>TM</sup> dart tags inserted into the musculature, below the second dorsal fin. In addition, 2,741 yellowfin and 2,443 bigeye were also chemically tagged with oxytetracycline (OTC), an antibiotic that is rapidly incorporated into calcified parts such as bones, scales, and otoliths and leaves a permanent fluorescent mark in the growth increment being formed at the time of tagging. According to fish size, 1.5-3 mL of OTC were injected with a syringe in the intramuscular part of their back (Hallier, 2008).

Recovery operations took place in the whole basin of the Indian Ocean during 2005-2012. Most of the reported recoveries came from fish caught by the European purse-seine (IOTC 2011). In September 2012, 10,395 yellowfin and 5,639 bigeye had been recovered (Figure ??).  $F_L$  of recovered fish was measured with caliper or tape measure to the nearest 0.5 cm. The accuracy in date and location of recaptures is dependent on place and process in which the tag is recovered. About 20% of the recoveries were made during purse seine fishing operations which resulted in the recovered fish to be associated with one position and date. By contrast, tunas recovered during purse seine unloading could be associated with several dates and locations of catch due to the process of storing tunas in refrigerated wells which contain about 5 sets over a fishing trip. The recovery can also occur downstream of the unloading process or in the canneries. The range of dates associated with each recapture was derived from logbook data and well maps through close collaboration between the IOTC and the purse seine fishing industry.

Some selection criteria have been applied to this mark-recapture data leading to a reliable dataset:

- Fish for which length measurement at tagging was considered unreliable by RTTP-IO team were excluded
- Fish for which the species recorded at tagging differs from the species at recovery were excluded.
- At tagging, all fish are measured in fork length whereas at recovery the length measurement may correspond to fork length, first dorsal length or curve length, the two latter being converted in fork length. This conversion is considered imprecise so these data were excluded.
- Fish for which length measurement at recovery was reported as unreliable were excluded.
- Fish with a negative growth rate between tagging and recapture were excluded.
- Fish whose date of recovery was unknown or known with low accuracy, i.e.  $> 5\%$ , were excluded.

- The dart-tagged fish that spent less than 90 days at sea and the OTC-tagged fish that spent less than 30 days at sea were excluded.
- The tag recovery system has evolved over the RTTP-IO program. Dates, positions and size measurements of recovery prior to 2007 being considered as low reliable, these observations have not been preserved.

Additional selection criteria was applied to obtain a dataset composed of 2,068 yellowfin and 2,655 bigeye (Table 1), i.e. only the yellowfin for which the exact recapture date and the bigeye for which the recapture date was known with an uncertainty of 7 days was used.

Table 1: Summarize of RTTP-IO data selections, \* Correspond to chemically tagged fish with oxytetracycline (OTC)

		Yellowfin		Bigeye	
Number of tagged fish	All data	66,534	2,756*		
	Selected tagging data	64,323	2,741*		
Number of recaptured fish	All data	10,505	257*		
	Selected tagging data	10,395	256*		
	Selected recovery data	4,464	174*		
	Data used	2,068	128*	2,655	85*

### 2.1.2 Direct ageing data

Currently, 256 yellowfin and 192 bigeye tagged with OTC have been recaptured. Sagittal otoliths were collected for ageing from 128 yellowfin, of 43 to 72 cm  $F_L$  at tagging and 47.9 to 135.4 cm  $F_L$  at recapture and from 85 bigeye of 44 to 71.5 cm  $F_L$  at tagging and 46 to 141.6 cm  $F_L$  at recapture. Otoliths were extracted, rinsed in water to remove tissue, and stored dry.

For the yellowfin, additional information to the RTTP-IO data were included: (i) 18 fish of 19 to 29 cm  $F_L$  captured during the tagging operations of the West Sumatra Tuna Tagging Project (WSTTP) carried out by the IOTC August 2007 and (ii) 42 fish captured in 2008 and 2009 by the Indian Ocean Tuna Ltd (IOT) including 7 males of 123.1 to 145 cm  $F_L$ , 7 females of 94.1 to 147.5 cm  $F_L$  and 28 indeterminate fish of 31 to 128.7 cm  $F_L$ .

Yellowfin have fragile, thin, and elliptic otoliths that require particular care during preparation and interpretation of microstructural features (Wild and Foreman, 1980). All otoliths collected were analysed at the "Laboratoire de Sclérochronologie des Animaux Aquatiques" (LASAA) in Brest, France. Otoliths were prepared for age analysis following methods described elsewhere (Secor et al., 1991; Stéquent, 1995; Panfili et al., 2002). They were cleaned in sodium hypochlorite and rinsed with distilled water before being embedded in resin block and transversally cut on both sides of the nucleus. The section containing the nucleus was then fixed to a glass slide using thermoplastic glue

and sanded to the level of the nucleus using different alumina grains (0.3 to 3  $\mu\text{m}$ ). The operation was performed on each side of the section until a slice of about 100  $\mu\text{m}$  thickness was decalcified with EDTA (tri-sodium-ethylene-diaminetetraacetic acid) to increase contrast between increments. The thin slides were examined under a microscope (1000x magnification) for counting increments throughout the counting path on the sagitta, i.e. from the primordium, or point of original growth, to the last increment deposited on a maximal growth axis.

Otoliths collected from fishes not chemically tagged were read in full, i.e. between the nucleus and edge (*Ir*). For the OTC-tagged yellowfin, the number of increments was counted for different otolith sections: (i) between nucleus and OTC mark (*It*), (ii) between the OTC mark and edge (*Im*) and (iii) between the nucleus and edge (*Ir*) (Fig. 1). For the OTC-tagged bigeye, the number of increments was counted for the sections *Im* and *It*. Each otolith was read 2-5 times without prior knowledge on size or time-at-liberty of the individuals sampled so as to maintain certain independence between the multiple readings. Otolith readings were performed by two reader teams.

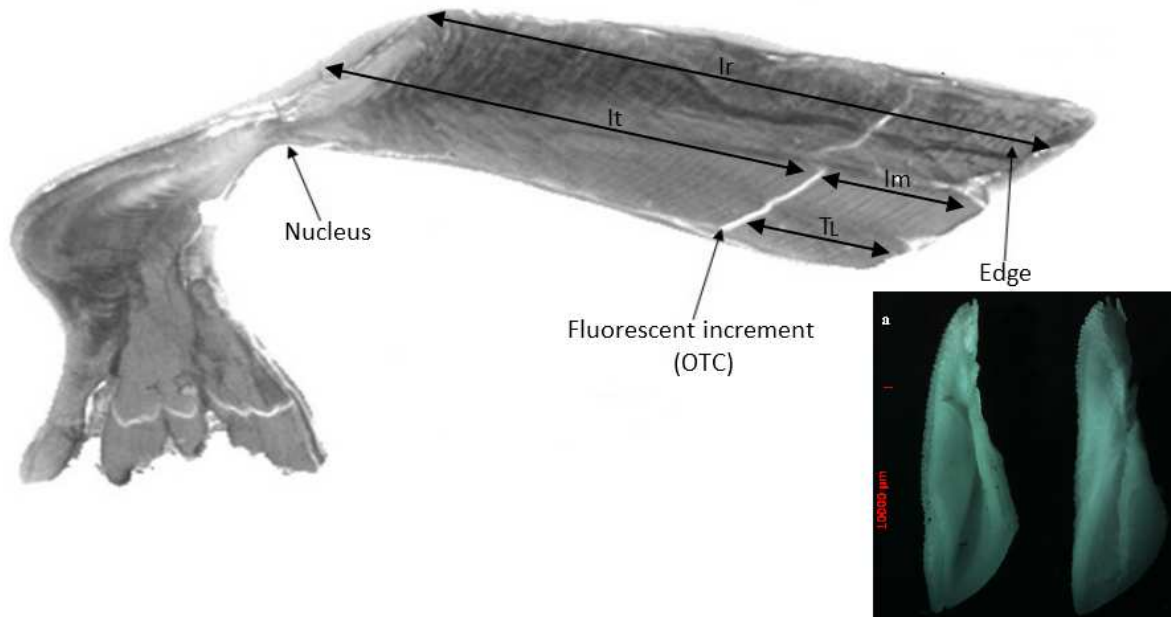


Figure 1: Otoliths of yellowfin tuna (external right and internal left) and the different sections used for reading the number of increments; OTC: Oxytetracycline; *It*: section from the nucleus to the OTC mark; *Im*: section from the OTC mark to the edge; *Ir*: section from the nucleus to the edge; *T<sub>L</sub>*: Time-at-Liberty

### 2.1.3 Modal progression from length-frequency data

Length-frequency data come from the "Balbaya" database managed by the "Institut de Recherche pour le Développement" (IRD, Sète) and correspond to commercial catches of European, Seychelles, Iranian and Mayotte purse-seine vessels. These catches were conducted under FAD-associated school

and free school between December 2000 and March 2010 in three fishing areas, i.e. Southeast and Northwest Seychelles and Sud Somali (Fig. 2).

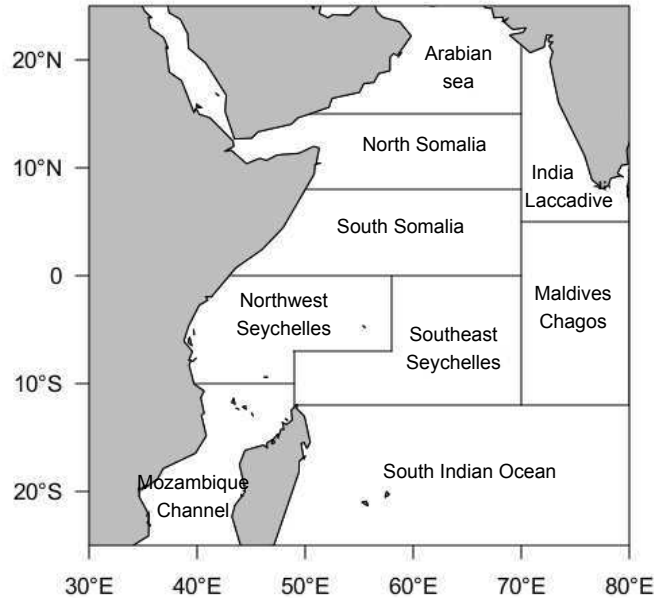


Figure 2: Fishnig areas of Indian Ocean

These length-frequency distributions exhibit various modes corresponding to different cohorts whose the progression in length was tracked monthly. An analytical method of modes separation was used. This latter describes the length distributions of the various cohorts, in a given month, as a mixture of normal distributions (Hasselblad, 1966; Schnute and Fournier, 1980). The modal determination was performed with the mix function, mixdist package of R statistical software version 2.12.2, that fits a set of overlapping component distributions to monthly length-frequency histograms using an Expectation-Maximization algorithm (Macdonald and Green, 1988). This function requires starting values for means and standard deviations. To optimize their choice, the normalmixEM function of mixtools package was used. Owing to a slower growth for larger fish and an increase of individual variability in size-age relationship with increasing age, especially after the sexual maturity, overlaps between successive length-at-age distributions increases and makes the visually identification of modes increasingly difficult. So, the standard deviation was constrained to increase with the mean value.

Yellowfin and bigeye have a seasonal sexual activity and thus display conspicuous recruitment peaks. The Indian Ocean yellowfin has two spawning season, the main from November to March with a peak in January and a minor period, involving a smaller number of spawning females, from June to August with a peak in June-July (Stéquent et al., 2001; Zhu et al., 2008). The juveniles are mainly recruited during August to October and February to March. The reproduction of bigeye occurs in

December to January and around June (Nootmorn, 2004) and the juveniles are mainly recruited during August to September and January to March. Therefore, an average age with an uncertainty of 3-4 months can be attributed to length modes. 23 cohorts and 16 cohorts were identified for yellowfin and bigeye respectively. But, due to lack of fish in intermediate sizes, it was impossible to follow the cohorts over 73 cm  $F_L$  for yellowfin and 115 cm  $F_L$  for bigeye (Fig. 3).

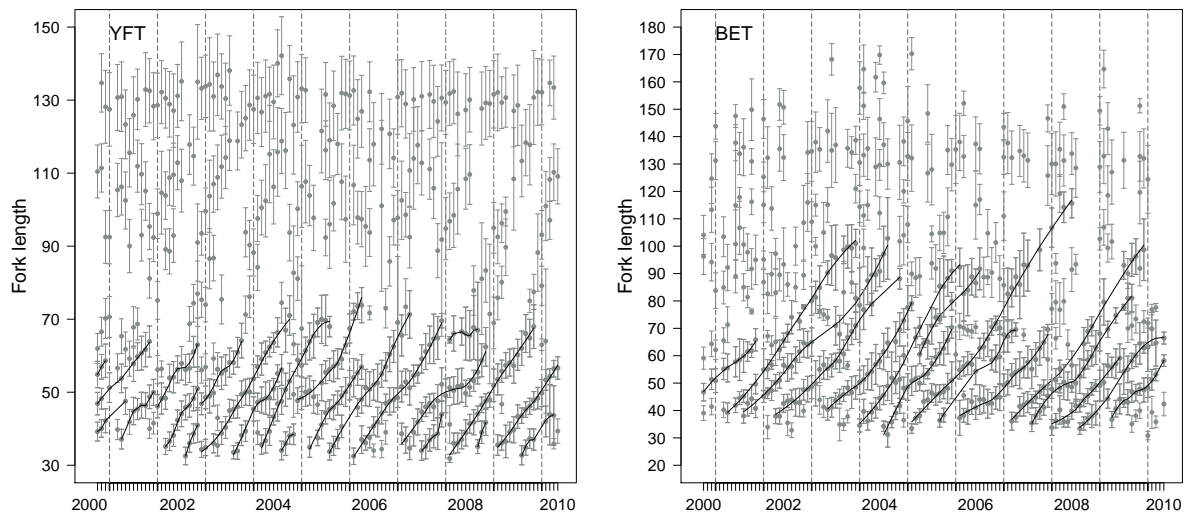


Figure 3: Monthly modal position in length-frequencies from purse seiners catches for yellowfin (YFT) and bigeye (BET). The circles represent the mode position and the vertical line the standard deviation; the solid curves correspond to the identified cohorts

## 2.2 Modelling growth

### 2.2.1 Choice of growth model

A hierarchical Bayesian model in which growth varies according to an individual-specific stochastic process was implemented. Preliminary analysis of the RTTP-IO data (Eveson and Million, 2008; Fonteneau and Gascuel, 2008) indicated a succession of phases of growth deceleration and acceleration in the growths of yellowfin and bigeye tunas. So, we considered the VB logK model, a two-stanza growth model developed by Laslett et al. (2002) for the growth of southern bluefin tuna. This model allows a smooth transition between two different growth rate coefficients ( $k_1$  and  $k_2$ ) through modeling changes in growth by a logistic function (Laslett et al., 2002; Eveson et al., 2004). The expected fork length at age  $A$  is expressed as:

$$f(A - t_0, \theta_g) = L_\infty (1 - \exp(-k_2(A - t_0))) \times \left( \frac{1 + \exp(-\beta(A - t_0 - \alpha))}{1 + \exp(\beta\alpha)} \right)^{\frac{(k_1 - k_2)}{\beta}} \quad (1)$$

All parameters used in this relation are defined in Table 2.

Table 2: Parameters and variables used in the somatic growth models

Variable	Definition
$L_{i,j}$	Fork length, i.e. length from the front to the fork in the center of the tail, for fish $i$ at opportunity of capture $j$ (cm)
$A_{i,j}$	Age of fish $i$ at opportunity of capture $j$ (y)
$mu_{c,k}$	Fork length mode for cohorte $c$ at month $k$ (cm)
$a_{c,1}$	Initial age for the cohorte $c$ (y)
$L_{\infty}$	Asymptotic fork length (cm)
$L_{\infty F}, L_{\infty M}$	Asymptotic fork length (cm) of females and males respectively
$L_{\infty M}$	Males asymptotic fork length (cm)
$k_1$	Juvenile growth rate coefficient ( $y^{-1}$ )
$k_{1F}, k_{1M}$	Juvenile growth rate coefficient ( $y^{-1}$ ) of females and males respectively
$k_2$	Adult growth rate coefficient ( $y^{-1}$ )
$k_{2F}, k_{2M}$	Adult growth rate coefficient ( $y^{-1}$ ) of females and males respectively
$\alpha$	Inflection point between the 2 stanzas (y)
$\beta$	Transition rate between $k_1$ and $k_2$
$t_0$	Theoretical age at fork length 0 (y)
$\varepsilon_{i,j}$	Length measurement error for fish $i$ at opportunity of capture $j$ (cm)
$\varepsilon_{\mu c,k}$	Modal length uncertainty for the cohort $i$ at time $k$
$\lambda_i$	Adjustement parameters for mark-recapture data

### 2.2.2 Fitting to direct ageing data

The tunas otoliths are particular difficult to read and the age estimation involves subjective interpretations of reader and comprises some uncertainties which can result in bias in growth estimate. Errors in interpreting and counting daily increments can first be related to otolith preparation for reading. In particular, some increments may be “lost“ at the otolith nucleus (i.e. core) and edge. Otoliths can also exhibit discontinuities and zones of overlap that result in some increments being omitted or counted more than once. Reading errors generally increase for older fish because the number of increments to count increases and because increments tend to get narrower with the distance from the nucleus when the fish is approaching its asymptotic length (Uchiyama and Struhsaker, 1981; Stéquent, 1995). In addition, growth increments might not always be consistently deposited daily, i.e. sub-daily increments and discontinuities in accretion rate may occur due to stress, reproduction, and environmental conditions, which may result in biased age estimates (Radtke and Fey, 1996; Panfili et al., 2009).

Therefore, a ageing error was used to estimate the individual ages of fish (?). Developed in a Bayesian framework, it explicitly considered the sources of uncertainty associated with otolith reading. In a first model step, the hypothesis of daily increment deposition (Wild and Foreman, 1980; Wild et al., 1995) was tested based on a subset of data of OTC-tagged otoliths. The information on the process of increment deposition was subsequently used in a second step for estimating the age of each fish based on counts of otolith increments. Expert judgment was included in the ageing error model through the choice of stochastic error structure and elicitation of informative prior density functions.

The somatic VB-logK growth model (Eq.11) was coupled to the ageing error model so as to propagate age uncertainty into growth parameter estimates and fitted to the data using Bayesian inference. The observed fork length of fish  $i$  at the opportunity of capture  $j$ , i.e;  $j = 1$  at tagging and  $j = 2$  at recapture, was then modeled as:

$$L_{i,j}^* = L_\infty(1 - \exp(-k_2(A_{i,j}^* - t_0))) \times \left( \frac{1 + \exp(-\beta(A_{i,j}^* - t_0 - \alpha))}{1 + \exp(\beta\alpha)} \right)^{\frac{(k_1 - k_2)}{\beta}} + \varepsilon_{i,j} \quad (2)$$

where the length measurement errors  $\varepsilon_{i,j}$  were assumed to be independent and normally distributed around zero with a common variance  $\sigma_{\varepsilon_j}^2$ .

Consider  $\theta_{g1} = \{L_\infty, k_1, k_2, t_0, \alpha, \beta\}$  the vector of growth parameters,  $\theta_a$  the vector of ageing parameters. Let  $I_{i,j}^*$  the number of counted increments for fish  $i$  at time  $j$ , i.e. either at tagging or at recapture,  $\pi[\theta_{g1}|L_{i,j}^*, A_{i,j}]$ ,  $\pi[\theta_a|I_{i,j}^*]$ , denote the posterior distributions of the parameters and  $\pi[\theta_{g1}]$ ,  $\pi[\theta_a]$ ,  $\pi[p]$  denote their prior distributions. Here,  $A_{i,j}$  are not directly observable latent variables. The full model corresponds to the joint distribution of parameters and latent variables.  $L_{i,j}^*$  and  $I_{i,j}^*$  being independent, this joint posterior distribution can written as:

$$\pi[\theta_{g1}, \theta_a | L_{i,j}^*, I_{i,j}^*] \propto \pi[L_{i,j}^*, A_{i,j} | \theta_{g1}] \times \pi[I_{i,j}^* | A_{i,j}, \theta_a] \times \pi[\theta_{g1}] \times \pi[\theta_a] \quad (3)$$

where  $\pi[L_{i,j}^*, A_{i,j} | \theta_{g1}]$  represents the conditional gaussian likelihood of observed lengths. Thus, the length values were predicted from the joint density:

$$f(L_j^* | I_{i,l}^*, \theta_{g1}) = \int \pi[L_{i,j}^* | A_{i,j}, \theta_{g1}] \times \pi[A_{i,j} | I_{i,j}^*, \theta_a] . dA_{i,j} \quad (4)$$

The product of the joint densities over all fish gives the likelihood function for the direct ageing data, and the negative likelihood was expressed as:

$$-ln(\mathcal{L}_1) = - \sum_i \sum_j f(L_{i,j}^* | I_{i,j}^*, \theta_{g1}) \quad (5)$$

### 2.2.3 Fitting to mark-recapture data

In markrecapture data, a fish of length  $L_1$  was tagged and released at time  $t_1$  and then recaptured at time  $t_2$  with length  $L_2$ . The change in fish size over the time interval  $[t_2, t_1]$  called time-at-liberty ( $T_L$ ) is a monotone increasing function of time expressed as follows (Wang, 1998):

$$L(t_2) = L(t_1) + (L_\infty - L(t_1)) \times (1 - \exp(-K(t_1, t_2))) \quad \text{with} \quad K(t_1, t_2) = \int_{t_1}^{t_2} k(t) . dt \quad (6)$$

$k(t)$  is the logistic function controlling the change in growth. From this form, we can express the length  $L_2$  as a function of  $L_1$  and  $T_L$  for each fish  $i$ :

$$L_{i,2}^* = L_{i,1}^* + (L_\infty - L_{i,1}^*) (1 - \exp(-k_2 \times T_{Li}^*)) \times \left( \frac{1 + \exp(-\beta(t_1 + T_L^* - t_0 - \alpha))}{1 + \exp(-\beta(t_1 - t_0 - \alpha))} \right) \frac{(k_1 - k_2)}{\beta} + \varepsilon_{i,2} \quad (7)$$

where  $t_1$  refers to the age at tagging. In mark-recapture data, the absolute age of fish is unknown and therefore these data provide no information to estimate the parameters  $\alpha$  and  $t_0$ . Let  $t_1 = 0$ ,  $\alpha_r = \alpha - t_1$  and  $t_{0r} = t_0 - t_1$ . We defined a new parameter  $\lambda$  as  $\lambda = \alpha_r + t_{0r}$ .  $\lambda$  varied from one fish to another because the fish are spawned at different times and they do not grow all at the same rate. Thus, the VB log K model (Eq. 11) for mark-recapture data had the following form:

$$L_{i,2}^* = L_{i,1}^* + (L_\infty - L_{i,1}^*) (1 - \exp(-k_2 \times T_{Li})) \times \left( \frac{1 + \exp(-\beta(T_{Li} - \lambda_i))}{1 + \exp(\beta \times \lambda_i)} \right) \frac{(k_1 - k_2)}{\beta} + \varepsilon_{i,2} \quad (8)$$

The  $\lambda_i$  parameters were used to relax the constraint on the anchor the growth curve which increase model flexibility. The joint posterior distribution of mark-recapture model was written as:

$$\pi[\theta_{g2}, \lambda_{ri} | L_{i,2}^*, L_{i,1}^*, T_{Li}^*] \propto \pi[L_{i,2}^*, L_{i,1}^*, T_{Li}^* | \theta_{g2}, \lambda_{ri}] \times \pi[\theta_{g2}] \times \pi[\lambda_{ri}] \quad (9)$$

where  $\theta_{g2} = \{k_1, k_2, \beta\}$ , and its negative likelihood as:

$$-\ln(\mathcal{L}_2) = - \sum_i f(L_{i,2}^* | L_{i,1}^*, T_{Li}^*, \theta_{g2}, \lambda_{ri}) = - \sum_i \int \pi[L_{i,2}^*, L_{i,1}^*, T_{Li}^* | \theta_{g2}, \lambda_{ri}] \cdot dL_{i,1}^* \cdot dT_{Li}^* \quad (10)$$

#### 2.2.4 Fitting to modal progression data

The modal progressions estimated from length-frequency distribution can be treated as multiple mark-recapture events where the initial age would be known. Let  $\mu_{i,k}$  the length mode value for the cohort  $c$ , equated with a fish, at the time  $k$ , equated with the opportunity of capture, and let  $a_{c,1}$  the mean age for the first mode. The time interval between two successive length modes, here one month, is denoted by  $d$ . The corresponding mean age for the length mode  $\mu_{c,k}$  is  $a_{c,k} = a_{c,1} + (k - 1)d$ . Thus, from Eq.11:

$$\mu_{c,k}^* = L_\infty (1 - \exp(-k_2(a_{c,1}^* + (k-1)d - t_0))) \times \left( \frac{1 + \exp(-\beta(a_{c,1}^* + (k-1)d - t_0 - \alpha))}{1 + \exp(\beta\alpha)} \right)^{\frac{(k_1 - k_2)}{\beta}} \times \varepsilon_{\mu c, k} \quad (11)$$

where  $\varepsilon_{\mu c, k}$  are the uncertainty on the modal length. They were assumed to be independent and normally distributed around zero with a common variance  $\sigma_\mu$ . Owing to a slower growth and an increase of individual variability in size-age relationship with increasing age (especially after the sexual maturity), overlaps between two successive length-at-age distributions increases and makes the identification of modes increasingly difficult. So, we considered here a multiplicative error.

The joint posterior distribution of modal progressions model was written as:

$$\pi[\theta_{g3} | \mu_{c,k}^*, a_{c,1}^*] \propto \pi[\mu_{c,k}^*, a_{c,1}^* | \theta_{g3}] \times \pi[\theta_{g3}] \quad (12)$$

where  $\theta_{g3} = \{L_\infty, k_1, k_2, t_0, \alpha, \beta, \sigma_\mu\}$ , and its negative likelihood as:

$$-\ln(\mathcal{L}_3) = - \sum_i f(\mu_{c,k}^* | a_{c,1}^*, \theta_{g3}) = - \sum_i \int \pi[\mu_{c,k}^*, a_{c,1}^* | \theta_{g3}] \cdot da_{c,1}^* \quad (13)$$

#### 2.2.5 Bayesian fit of integrated growth model

The three data sources being independent, the overall negative log-likelihood is the sum of the log-likelihood defined in Eqs. 5, 10 and 13:

$$-\ln(\mathcal{L}) = -(\ln(\mathcal{L}_1) + \ln(\mathcal{L}_2) + \ln(\mathcal{L}_3)) \quad (14)$$

The integrated growth model was fitted to the data using a Bayesian inference. In a Bayesian framework, the parameters  $\theta$  are treated as random variables and a prior probability distribution is their assigned (Table 3). This offers the possibility of introducing expert knowledges in the model. The asymptotic length  $L_\infty$  is a particularly important parameter because it determines the shape of the second part of the growth curve. Since the data set included little information on the asymptotic part of the growth curve, auxiliary information was provided for this parameter consistently with the available knowledge on the biology of the species. An informative prior distribution was defined for  $L_\infty$  through the use of a generalized extreme value distribution (GEV), which allows extrapolation of the distribution tails behavior from the greatest values of a sample and thus estimates the occurrence probability of extreme events (Borchani, 2010). The choice of this distribution is motivated by the fact that tunas grow throughout their life so that the largest observed sizes should correspond to the oldest fish. The distribution was fitted based on size measurement data on fresh fish collected during 1952-2011 from the European and Seychelles purse seine fisheries, Maldivian pole and line vessels, and Taiwanese and Japanese longliners.

The growth rate coefficients  $k_1$  and  $k_2$  are in part model-specific and weakly informative priors were assigned to them.  $k_1$  was assumed to vary according to a gamma prior distribution with mean and coefficient of variation determined from the literature.  $k_2$  was set equal to  $k_1 + \kappa$  with  $\kappa$  following a uniform distribution (Tables ?? and ??).

The transition rate  $\beta$  between  $k_1$  and  $k_2$  which is specific to the VB-logK model and the theoretical age of zero length  $t_0$  that depends on the data were assigned weakly informative distributions.

The parameter  $\alpha$  is the mean age relative to  $t_0$  at which change in growth occurs and was assigned a weakly informative prior gamma distribution with mean defined from the literature on yellowfin growth (Gascuel et al., 1992; Lehodey and Leroy, 1999; Lumineau, 2002; Viera, 2005). For the big-eye, no prior information was available in the literature. However, this species being physiologically close to yellowfin, we have supposed that the same prior might be used.

The standard deviation of size measurement errors  $\sigma_{\epsilon_j}$  was determined from fork length differences of RTTP-IO fishes released and recaptured several times with time-at-liberties less than or equal to 7 days. These individuals were not included in subsequent analyses and therefore constitute an independent data set. On the other hand, some recapture lengths were measured on frozen fish, that may include a bias due to tuna shrinkage: frozen fish in brine are often severely compressed. This "shrinkage" bias was estimated from some fish that have been thawed and remeasured with a good precision. But, the length could as well be overestimated or underestimated. Preliminary analysis showed that the model results were very sensitive to specification of prior on measurement errors. In addition, the model proved unable to estimate these errors when a uninformative prior was used. Thus, to obtain consistent results, the standard deviation values  $\sigma_{\epsilon_j}$  was fixed to 3 at tagging and 5 at recapture.

The standard deviation of modal length errors  $\sigma_\mu$  was unknown and an uninformative inverse gamma distribution their assigned.

$\lambda_i$  are adjustment parameters and uniform distributions defined on the interval  $[-5; 5]$  have been assigned.

The initial mean ages  $a_{c,1}$  were estimated with a precision of 3-4 months and were distributed around the estimated age according to a gamma distribution.

Estimates of age and growth parameters were evaluated from three Markov Chain Monte Carlo (MCMC) simulations using a Gibbs sampler as implemented in OpenBugs version 3.2.1 (Spiegelhalter et al., 2011). The convergence of the MCMC to stationary posterior distribution was evaluated from the Gelman-Rubin diagnostic, based on the ratio of inter-chain variance on intra-chain variance. It must be close to 1 for getting convergence (Gelman and Rubin, 1992). Convergence is reached when the influence of the likelihood dominates the prior information resulting in indistinguishable chains outputs. This diagnostic is computed from second half of MCMC simulation samples.

Table 3: Prior distribution used for parameters of somatic growth models. All variables are defined in Table

Yellowfin	Bigeye
$L_\infty \sim GEV(173.141, 11.067, -0.3474)$	$L_\infty \sim GEV(187.622, 9.189, -0.3313)$
$k_1 \sim \Gamma(2.778, 0.211)$	$k_1 \sim \Gamma(4, 0.058)$
$k_2 = k_1 + \kappa$ with $\kappa \sim \mathcal{U}(0, 3)$	$k_2 = k_1 + \kappa$ with $\kappa \sim \mathcal{U}(0, 3)$
$\alpha \sim \Gamma(25, 1)$	$\alpha \sim \Gamma(25, 1)$
$\beta \sim \Gamma(4, 6.826)$	$\beta \sim \mathcal{U}(0, 30)$
$t_0 \sim \mathcal{U}(-2, 0)$	$t_0 \sim \mathcal{U}(-2, 0)$
$\varepsilon_{i,j} \sim \mathcal{N}(0, \sigma_{\varepsilon_j}^2)$ with $\sigma_{\varepsilon_j}$ fixed to 3 at tagging and to 5 at recapture	
$\varepsilon_{\mu c,j} \sim \mathcal{N}(0, \sigma_\mu^2)$ with $\sigma_\mu \sim Inv\Gamma(0.04, 0.01)$	

### 3 Results

For both integrated growth models, that of yellowfin and that of bigeye, the Gelman-Rubin diagnostic of each parameters, computed from second half of MCMC simulation samples, was closed to 1.0, indicating convergence. The values of multivariate potential scale reduction factor were 1.03 and 1.09 for the yellowfin model and bigeye model respectively.

he model supported a two-stanza growth for yellowfin of the Indian Ocean with 2 distinct phases over the fish lifespan (Figure 4). The first stanza was characterized by a relatively slow growth, which gradually decreased to a minimum of 1.43 cm.month<sup>-1</sup> up to 1.8 years (around 62 cm  $F_L$ ). It was followed by a second stanza in which the growth accelerated up to a maximum of 4.02 cm.month<sup>-1</sup> until 2.46 years (81 cm  $F_L$ ) and then progressively decreased with size to become very slow when size was close to the asymptotic length, reaching 0.01 cm.month<sup>-1</sup> around 145 cm  $F_L$ . The mean

age at which change in growth occurs was estimated between 2.25 y, corresponding to about 73 cm  $F_L$ . The mean growth rates were about 1.73 cm.month<sup>-1</sup> from 30 to 65 cm  $F_L$ , 2.02 cm.month<sup>-1</sup> from 65 to 80 cm  $F_L$  and 1.84 cm.month<sup>-1</sup> from 80 to 155 cm  $F_L$ . The mean age at which change in growth occurs was estimated at 2.25 y, corresponding to about 73 cm  $F_L$ . The mean population asymptotic length was estimated between 142.6 cm  $F_L$  and 150 cm  $F_L$  (5), which was lower than the maximal observed length of 159 cm  $F_L$ . This value was very low comparatively to the mean asymptotic fork length estimated at about 173 cm from the catch of the purse seiners and longliners and to the maximum lengths of 200 cm that have been observed for yellowfin in the Indian Ocean.

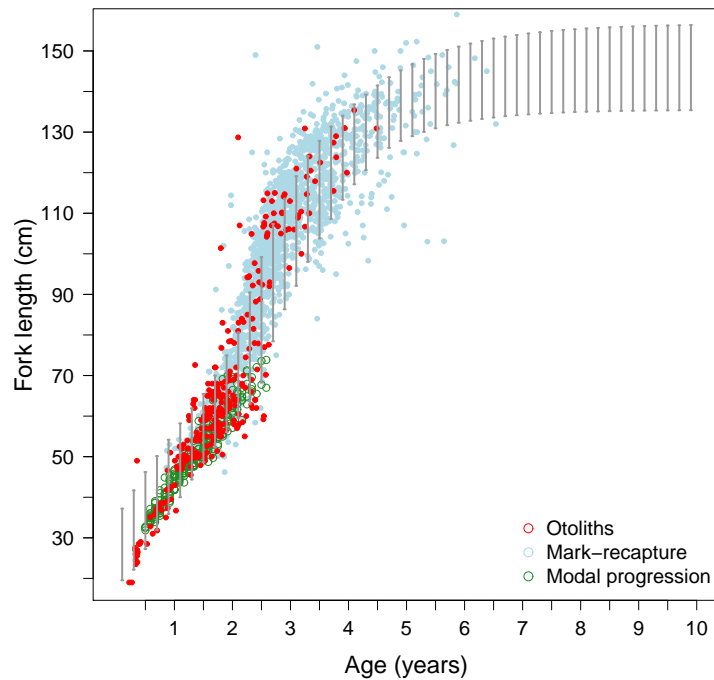


Figure 4: Yellowfin growth curve as estimated from the integrated model

Bigeye also showed a two-stanza growth with a less pronounced transition than yellowfin. Nevertheless, the model underestimated the growth in the second stanza (Figure 5). The convergence was difficult to reach. This may be partly related to contradictions in the data, in particular in age reading data.

Table 4: Attributes of marginal posterior distributions from yellowfin integrated VB log K growth model

Parameters	Mode	Mean	Standard deviation	Posterior quantiles	
				2.5%	97.5%
$L_\infty$ (cm)	145.543	145.88	1.9	142.597	150.002
$\alpha$ (years)	3.104	3.166	0.14	2.983	3.533
$\beta$	6.692	16.653	14.73	2.436	58.93
$k_1$ (years <sup>-1</sup> )	0.207	0.204	0.01	0.182	0.22
$k_2$ (years <sup>-1</sup> )	0.797	0.799	0.035	0.729	0.866
$t_0$ (years)	-0.884	-0.919	0.086	-1.117	-0.791
$\sigma_\mu$ (cm)	0.048	0.049	0.003	0.044	0.055

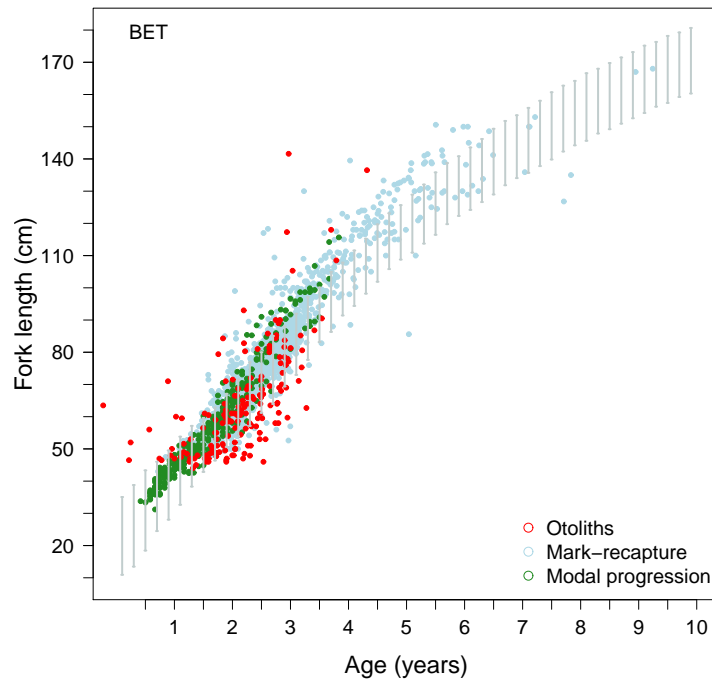


Figure 5: Bigeye growth curve as estimated from the integrated model

## References

- Borchani, A. (2010). Statistiques des valeurs extrêmes dans le cas de lois discrètes. Technical Report ESSEC Working Paper 10009, ESSEC Business School.
- Chantawong, P., Panjarat, S., and Singtongyam, W. (1999). Preliminary results on fisheries and biology of bigeye tuna (*Thunnus obesus*) in the eastern Indian Ocean. *IOTC Proceedings*, 12(2):231–241.
- Chen, Y., Jiao, Y., and Chen, L. (2003). Developing robust frequentist and Bayesian fish stock

Table 5: Attributes of marginal posterior distributions from bigeye integrated VB logK growth model

Parameters	Mode	Mean	Standard deviation	Posterior quantiles	
				2.5%	97.5%
$L_\infty$ (cm)	214.219	213.456	1.35	209.695	215.1
$\alpha$ (years)	3.635	3.563	0.297	2.508	3.897
$\beta$	10.015	15.997	8.95	4.59	39.249
$k_1$ (years <sup>-1</sup> )	0.106	0.106	0.004	0.1	0.119
0.104					
$k_2$ (years <sup>-1</sup> )	0.172	0.171	0.005	0.157	0.178
$t_0$ (years)	-1.132	-1.121	0.114	-1.302	-0.744
$\sigma_\mu$ (cm)	1.07	1.071	0.005	1.063	1.081

assessment methods. *Fish and Fisheries*, 4:105–120.

Clark, J. S. (2005). Why environmental scientists are becoming Bayesians. *Ecology Letters*, 8(1):2–14.

Cressie, N., Calder, C., Clark, J., Ver Hoef, J., and Wikle, C. (2009). Accounting for uncertainty in ecological analysis: the strengths and limitations of hierarchical statistical modeling. *Ecological Applications*, 19(3):553–570.

Eveson, J. and Million, J. (2008). Estimation of growth parameters for yellowfin, bigeye and skipjack tuna using tag-recapture data. *IOTC-Working Party on Tagging Data Analysis*, 7(07):31p.

Eveson, J. P., Laslett, G. M., and Polacheck, T. (2004). An integrated model for growth incorporating tag-recapture, length-frequency, and direct aging data. *Canadian Journal of Aquatic and Fisheries Sciences*, 61:292–306.

Fonteneau, A. and Gascuel, D. (2008). Growth rates and apparent growth curves, for yellowfin, skipjack and bigeye tagged and recovered in the Indian Ocean during the IOTTP. *IOTC-WPTDA*, 8:23p.

Gascuel, D., Fonteneau, A., and Capisano, C. (1992). Modélisation d’une croissance en deux stances chez l’albacore (*Thunnus albacares*) de l’Atlantique Est. *Aquatic Living Resources*, 5:155–172.

Gelman, A., Carlin, J., Stern, H., and Rubin, D. (2004). *Bayesian Data Analysis, Second Edition*. Chapman & Hall/CRC Texts in Statistical Science, CRC press book edition.

Gelman, A. and Rubin, D. (1992). Inference from iterative simulation using multiple sequences. *Statistical Science*, 7(4):457–511.

Hallier, J. (2008). Status of the Indian Ocean tuna tagging programme - RTTP-IO. *IOTC-WPTDA*, 10:40p.

- Hasselblad, V. (1966). Estimation of parameters for a mixture of normal distributions. *Technometrics*, 8(3):431–444.
- Helser, T. and Lai, H.-L. (2004). A Bayesian hierarchical meta-analysis of fish growth: with an example for North American largemouth bass, *Micropterus salmoides*. *Ecological Modelling*, 178:399–416.
- Herrera, M. and Pierre, L. (2010). Status of IOTC databases for tropical tunas. *IOTC-WPTT*, 3:28p.
- Kume, S. and Joseph, J. (1966). Size composition, growth and sexual maturity of bigeye tuna, *Thunnus obesus* (Lowe), from the Japanese long-line fishery in the Eastern Pacific Ocean. *Inter-American Tropical Tuna Commission Bulletin*, 11(2):47–75.
- Langley, A., Herrera, M., and Million, J. (2010). Stock assessment of yellowfin tuna in the Indian Ocean using MULTIFAN-CL. *IOTC-WPTT*, 23:72p.
- Laslett, G., Eveson, J., and Polacheck, T. (2002). A flexible maximum likelihood approach for fitting growth curves to tag-recapture data. *Canadian Journal of Fisheries and Aquatic Sciences*, 59:976–986.
- Le Guen, J. and Sakagawa, G. (1973). Apparent growth of yellowfin tuna from the Eastern Atlantic ocean. *Fishery Bulletin*, 71(1):175–187.
- Lehodey, P. and Leroy, B. (1999). Age and growth of yellowfin tuna (*Thunnus albacares*) from the western and central Pacific Ocean as indicated by daily growth increments and tagging data. *12th Meeting of the SCTB, Working Paper YFT-2*, pages 1–21.
- Lumineau, O. (2002). Study of the growth of Yellowfin tuna (*Thunnus albacares*) in the Western Indian Ocean based on length frequency data. *IOTC Proceedings*, 5:316–327.
- Macdonald, P. and Green, P. (1988). User’s guide to program MIX: An interactive program for fitting mixtures of distributions. *Ichthus Data Systems*.
- Marsac, F. (1991). Preliminary study of the growth of yellowfin estimated from purse seine data in the Western Indian Ocean. *IPTP Collective volume of working documents*, 6:35–39.
- Marsac, F. and Lablache, G. (1985). Preliminary study of the growth of yellowfin estimated from purse seine data in the Western Indian Ocean. *IPTP Collective volume of working documents*, pages 91–110.
- McAllister, M., Pikitch, E., and Babcock, E. (2001). Using demographic methods to construct Bayesian priors for the intrinsic rate of increase in the Schaefer model and implications for stock rebuilding. *Canadian Journal of Fisheries and Aquatic Sciences*, 58:1871–1890.

- Nootmorn, P. (2004). Reproductive biology of bigeye tuna in the Eastern Indian Ocean. *IOTC Proceedings*, 7:1–5.
- Nootmorn, P., Yakoh, A., and Kawises, K. (2005). Reproductive biology of yellowfin tuna in the Eastern Indian Ocean. *IOTC-WPTT*, 14:379–385.
- Panfili, J., De Pontual, H., Troadec, H., and Wright, P. (2002). *Manuel de sclérochronologie des poissons*. Coédition Ifremer-IRD.
- Panfili, J., Tomas, J., and Morales-Nin, B. (2009). Otolith microstructure in tropical fish. In *Tropical fish otoliths: information for assessment, management and ecology*, Methods and Technologies in Fish Biology and Fisheries Volume 11: 212-248. Green B.S. et al. [Ed.].
- Punt, A. and Hilborn, R. (1997). Fisheries stock assessment and decision analysis: the Bayesian approach. *Reviews in Fish Biology and Fisheries*, 7:35–63.
- Radtke, R. and Fey, D. P. (1996). Environmental effects on primary increment formation in the otoliths of newly-hatched Arctic charr. *Journal of Fish Biology*, 48(6):1238–1255.
- Romanov, E. and Korotkova, L. (1988). Age and growth rates of yellowfin tuna *Thunnus albacares* (Bonnaterre 1788) (Pisces, Scombridae) in the north-western part of the Indian Ocean, determined by counting the rings of vertebrae. *FAO/IPTP Collection Volume of Working Documents*, 3:68–73.
- Schnute, J. and Fournier, D. (1980). A new approach to length-frequency analysis: growth structure. *Canadian Journal of Fisheries and Aquatic Sciences*, 37(9).
- Secor, D., Dean, J., and Laban, E. (1991). Manual for otolith removal and preparation for microstructural examination. *Electric Power Research Institute and the Belle W. Baruch Institute for Marine Biology and Coastal Research*.
- Spiegelhalter, D., Thomas, A., Best, N., and Lunn, D. (2011). OpenBUGS version 3.2.1 user manual.
- Stéquert, B. (1995). Détermination de l'âge des thons tropicaux à partir de leurs otolithes: exemple du Yellowfin (*Thunnus albacares*). *Document Technique du Centre ORSTOM de Brest*, 76:1–31.
- Stéquert, B. and Conand, F. (2004). Age and growth of bigeye tuna (*Thunnus obesus*) in the Western Indian Ocean. *Cybium*, 28(2):163–170.
- Stéquert, B., Rodriguez, J., Cuisset, B., and Le Menn, F. (2001). Gonadosomatic index and seasonal variations of plasma sex steroids in skipjack tuna (*Katsuwonus pelamis*) and yellowfin tuna (*Thunnus albacares*) from the Western Indian Ocean. *Aquatic Living Resources*, 14:313–318.
- Uchiyama, J. and Struhsaker, P. (1981). Age and growth of skipjack tuna, *Katsuwonus pelamis*, and yellowfin tuna, *Thunnus albacares* as indicated by daily growth increments of sagittae. *Fishery Bulletin*, 79:151–162.

- Viera, A. (2005). Study of the growth of Yellowfin tuna (*Thunnus albacares*) in the Indian Ocean based on length-frequency data from 2000 to 2004. *IOTC-WPTT*, 32:17p.
- Wang, Y.-G. (1998). Growth curves with explanatory variables and estimation of the effect of tagging. *Australian and New Zealand Journal of Statistics*, 40(3):299–304.
- Wild, A. (1986). Growth of yellowfin tuna, *Thunnus albacares*, in the Eastern Pacific Ocean based on otolith increments. *Inter-American Tropical Tuna Commission Bulletin*, 18(6):423–479.
- Wild, A. and Foreman, T. (1980). The relationship between otolith increments and time for yellowfin and skipjack tuna marked with tetracycline. *Inter-American Tropical Tuna Commission Bulletin*, 17(7):507–560.
- Wild, A., Wexler, J., and Foreman, T. (1995). Extended studies of increment deposition rates in otoliths of yellowfin and skipjack tunas. *Bulletin of Marine Science*, 57(2):555–562.
- Zhu, G., Xu, L., Zhou, Y., and Song, L. (2008). Reproductive Biology of Yellowfin Tuna *T. albacares* in the West-Central Indian Ocean. *Journal of Ocean University of China*, 7(3):327–332.
- Zudaire, I., Murua, H., Grande, M., Korta, M., Arrizabalaga, H., Areso, J., and Delgado-Molina, A. Reproductive biology of yellowfin tuna (*Thunnus albacares*).